Meccanica (2009) 44: 305–319
DOI 10.1007/s11012-008-9170-2

Lamb waves in micropolar thermoelastic solid plates immersed in liquid with varying temperature

J.N. Sharma · Satish Kumar

Received: 8 July 2007 / Accepted: 31 July 2008 / Published online: 10 October 2008

Abstract In the present paper the theory of micropolar generalized thermoelastic continua has been employed to study the propagation of plane waves in micropolar thermoelastic plates bordered with inviscid liquid layers (or half-spaces) with varying temperature on both sides. The secular equations in closed form and isolated mathematical conditions are derived and discussed. Thin plate and short wave length results have also been deduced under different cases and situations and discussed as special cases of this work. The results in case of conventional coupled and uncoupled theories of thermoelasticity can be obtained both in case of micropolar elastic and elastokinetics from the present analysis by appropriate choice of relevant parameters. The various secular equations and relevant relations have been solved numerically by using functional iteration method in order to illustrate the analytical developments. Effect of characteristic length and coupling factors have also been studied on phase velocity. The computer simulated results in case of phase velocity, attenuation coefficient and specific loss of symmetric and skew symmetric are presented graphically.

Keywords Micropolar · Interfacial waves · Generalized thermoelasticity · Characteristic length · Continuum mechanics

J.N. Sharma (✉)
Department of Applied Sciences, National Institute of Technology, Hamirpur 177 005, India
e-mail: jns@nitham.ac.in

S. Kumar
Department of Mathematics, Lovely Professional University, Phagwara 144001, India

1 Introduction

Classical continuum theories can explain the mechanical behavior of common solid material like coal, concrete etc. but it is unable to explain the behavior of complex materials such as bones, blood, cellular solids and polymers. The reason of the complexities lies in the microstructure of the materials. Therefore, micro-continuum theories were developed by considering a continuum model embedded with microstructure which can explain the microscopic motion and long range material interactions. Several attempts were made to explain these discrepancies that occur in the case of problems involving elastic vibrations of high-frequencies and short wave length, that is, vibrations due to the generation of ultrasonic waves. Voigt [1] attempted to eliminate these discrepancies by suggesting that transmission of interaction between two particles of a body through an elementary area lying within the material was affected not solely by the action of a force vector but also by a moment (couple) vector. This led to the concept of

couple stresses in elasticity. Cosserat [2] developed a non-linear theory of elasticity for bars, surfaces and bodies; Eringen and Şuhubi [3] and Mindlin [4] introduced non-linear micromorphic theory and linear microstructure respectively by extending classical elasticity to include the effects of the deformations of the underlying microstructure by inserting new degrees of freedom into the continuum. These degrees of freedom are specified to be independent from the usual displacement degrees of freedom. In the case of the micropolar continuum introduced by Eringen [5] the directors are rigid and there are three rotational degrees of freedom in addition to the three classical displacement degrees of freedom. Fatima et al. [6] suggested that the Cosserat continuum theory is a possible choice within the whole class of generalized continuum theories for the mechanical modeling of bone. Anderson and Lakes [7] showed that classical elasticity theory does not always adequately describe the behavior of cellular materials and they also proved that Rohacell polymethacrylimide foam behaves as a Cosserat elastic material. Some authors such as Di Carlo et al. [8] and Masiani et al. [9] showed how to obtain a macroscopic characterization of a continuum with a fine microstructure in masonry applications. Masiane and Trovalusci [10] showed that simplest kind of microstructure which can be used to describe masonry like material is the rigid microstructure of the Cosserat type.

In order to remove the paradox of infinite velocity of heat transportation; a physically impossible phenomenon, non-classical (generalized) theories of thermoelasticity have been developed by the authors such as Lord and Shulman [11] and Green and Lindsay [12]. Some researchers such as Ackerman et al. [13], Guyer and Krumhansal [14] and Ackerman and Overtone [15] experimentally proved for solid helium that thermal wave (second sound) propagating with finite, though quite large, speed also exists. A wave like thermal disturbance is referred to as "second sound" by Chandrasekharaiah [16]. Dost and Tabarrok [17] advanced the linear micropolar theory of elastic continua developed by Eringen [18] to generalized thermoelastic solids by using Green and Lindsay [12] model of non-classical thermoelasticity. Kumar and Choudhary [19] studied the response of orthotropic micropolar elastic medium due to various sources. The study of Lamb wave propagation in elastic plates under fluid loading carried out by Wu and Zhu [20] has been advanced by Sharma and Pathania [21] for thermoelastic plates immersed in liquid. This study was further extended to cylindrical thermoelastic plates sandwiched between fluid layers of finite and infinite thicknesses by Sharma and Pathania [22]. However, these investigations were subjected to the assumption that the liquid loading is maintained at uniform temperature, a constraint difficult to follow practically. Recently Sharma et al. [23] studied the propagation of Rayleigh surface waves in microstretch thermoelastic continua under inviscid fluid loadings with varying temperature.

The plate like structure is in frequent use in applications involving aerospace, navigation, civil engineering structures, chemical pipes, and automobiles etc. Moreover, capability of Lamb waves in interrogating complete plate like structure is quite useful in the structural health monitoring and for diagnostics of such structures.

Keeping in view the above facts the present paper is aimed at to investigate the Lamb wave phenomenon in micropolar thermoelastic solid plates submerged in liquid with varying temperature. The linear micropolar theory of elastic continua developed by Eringen [18] and advanced by Dost and Tabarrok [17] to generalized thermoelastic solids has been employed, to carry out the investigations.

2 Formulation of the problem

We consider a homogeneous isotropic, thermally conducting, cylindrical micropolar elastic plate of thickness $2d$ initially at uniform temperature T_0. The plate is bordered, both on the top and bottom, with infinitely large homogeneous inviscid liquid layers of thickness h. The plate is axisymmetric with respect to z-axis as the axis of symmetry. We use cylindrical coordinates to solve this problem. The origin of coordinate system (r, θ, z) is taken at any point in the middle surface of the plate and z-axis normal to it along the thickness. The surfaces $z = \pm d$ are subjected to stress/couple free, thermally insulated/isothermal boundary conditions. We take the r–z plane as the plane of incidence. The basic governing equations for micropolar thermoelastic medium developed by Eringen [15] and Dost and Tabarrok [17] after employing Lord and Shulman [11] and Green and Lindsay [12]

models of nonclassical thermoelasticity, in the absence of body forces and heat sources, are given by

$$(\lambda+\mu)\nabla(\nabla.\vec{u})+(\mu+\kappa)\nabla^2\vec{u}+\kappa\nabla\times\vec{\phi}-\nu\left(1+t_1\delta_{2k}\frac{\partial}{\partial t}\right)\nabla T=\rho\frac{\partial^2\vec{u}}{\partial t^2}, \tag{1}$$

$$(\alpha+\beta+\gamma)\nabla(\nabla\cdot\vec{\phi})-\nu\nabla\times(\nabla\times\vec{\phi})+\kappa(\nabla\times\vec{u})-2\kappa\vec{\phi}=\rho j\frac{\partial^2\vec{\phi}}{\partial t^2}, \tag{2}$$

$$K^*\nabla^2T=\rho C^*\left(\frac{\partial T}{\partial t}+t_0\frac{\partial^2T}{\partial^2t^2}\right)+\nu T_0\left(\frac{\partial}{\partial t}+\delta_{1k}t_0\frac{\partial^2}{\partial t^2}\right)(\nabla\cdot\vec{u}). \tag{3}$$

The constitutive relations are given by

$$\sigma_{ij}=\lambda u_{r,r}\delta_{ij}+\mu(u_{i,j}+u_{j,i})+\kappa(u_{j,i}-\in_{ijr}\phi_r)-\nu\left(T+t_1\delta_{2k}\frac{\partial}{\partial t}\right)\delta_{ij},$$

$$m_{ij}=\alpha\phi_{r,r}\delta_{ij}+\beta\phi_{i,j}+\gamma\phi_{j,i},\quad i,j,r=1,2,3 \tag{4}$$

where $\vec{u}=(u,0,w)$ is the displacement vector, T is temperature change, $\vec{\phi}=(0,\phi,0)$ is micro rotation vector. Here λ, μ are Lame parameters and γ, κ, α, β are micropolar material constants, ρ is density, K^* is thermal conductivity, $\nu=(3\lambda+2\mu+\kappa)\alpha_T$, α_T is coefficient of linear thermal expansion. σ_{ij} and m_{ij} are respectively the stress tensor and couple stress tensor and δ_{ij} is Kronecker delta. Here $k=1$ for Lord-Schulman (LS) theory and $k=2$ for Green-Lindsay (GL) theory. The comma notation is used to denote spatial derivative, a dot denotes time differentiation.

The thermal relaxation time 't_0' and 't_1' satisfy the inequalities

$$t_0\geq t_1\geq 0. \tag{5}$$

The inequalities (5) are not mandatory to be satisfied as proved by Strunin [24].

We have defined the quantities

$$r'=\frac{\omega^*r}{c_1},\qquad z'=\frac{\omega^*z}{c_1},\qquad T'=\frac{T}{T_0},$$

$$u'=\frac{\rho\omega^*c_1u}{\nu T_0},\qquad w'=\frac{\rho\omega^*c_1w}{\nu T_0},$$

$$t'=\omega^*t,\qquad t_0'=\omega^*t_0,\qquad t_1'=\omega^*t_1,$$

$$\varepsilon=\frac{\nu^2T_0}{\rho C^*}(\lambda+2\mu+\kappa),$$

$$\omega^*=\frac{C^*(\lambda+2\mu+\kappa)}{K},\qquad \sigma_{ij}'=\frac{\sigma_{ij}}{\nu T_0}, \tag{6}$$

$$\delta^2=\frac{c_2^2}{c_1^2},\qquad \delta_1^2=\frac{c_4^2}{c_1^2},$$

$$c_1^2=\frac{\lambda+2\mu+\kappa}{\rho},\qquad c_2^2=\frac{\mu+\kappa}{\rho},$$

$$c_3^2=\frac{K^*}{\rho C^*\omega^*},\qquad c_4^2=\frac{\gamma}{\rho J},$$

$$c_7^2=\frac{\kappa}{\rho J},\qquad p=\frac{\kappa}{\rho c_1^2},\qquad \delta^*=\frac{\kappa c_1^2}{\gamma\omega*^2}$$

ω^* is characteristic frequency of medium, c_1 and c_2 one longitudinal and shear velocity, C^* is specific heat.

Moreover Fatima et al. [6] defined the characteristic length (l) and coupling factor (N) for the material in terms of material parameters as

$$\gamma=4l^2\left(\mu+\frac{\kappa}{2}\right),\qquad N^2=\frac{\kappa}{2(\mu+k)} \tag{7}$$

where $0\leq N<1$. Here $N=0$ corresponds to a classical elastic material and $N=1$ refers to famous coupled stress theory.

Upon using (6) in (1) to (3) we obtain.

$$(1-\delta^2)\nabla(\nabla\cdot\vec{u})+\delta^2\nabla^2\vec{u}+p(\nabla\times\vec{\phi})-\left(1+t_1\delta_2k\frac{\partial}{\partial t}\right)\nabla T=\frac{\partial^2\vec{u}}{\partial t^2}, \tag{8}$$

$$\nabla^2\vec{\phi}+\delta^*(\nabla\times\vec{u})-2\delta^*\vec{\phi}=\frac{1}{\delta_1^2}\frac{\partial^2\vec{\phi}}{\partial t^2}, \tag{9}$$

$$\nabla^2T-\left(\frac{\partial}{\partial t}+t_0\frac{\partial^2}{\partial t^2}\right)T=\varepsilon\left(\frac{\partial}{\partial t}+\delta_{1k}t_0\frac{\partial^2}{\partial t^2}\right)(\nabla\cdot\vec{u}). \tag{10}$$

In order to solve above equations we introduce potential q and ψ, in the solid defined by

$$u=q_{,r}+\psi_{,z},\qquad w=q_{,z}-\psi_{,r}-\frac{\psi}{r}. \tag{11}$$

Also in the liquid boundary layer we have

$$u_j=\phi_{j,r}+\psi_{j,z},\qquad \omega_j=\phi_{j,z}-\psi_{j,r}-\frac{\psi_j}{r} \tag{12}$$

where ϕ_j and ψ_j are scalar velocity potential and vector velocity components, respectively along the direction for the bottom liquid layer ($j=1$) and top liquid layer ($j=2$), u_j and ω_j are the r and z components of particle velocity. Substituting (11), (12) in (8) to (10) we obtained

$$\left(\nabla^2-\frac{\partial^2}{\partial t^2}\right)q=\left(1+t_1\delta_{2k}\frac{\partial}{\partial t}\right)T, \tag{13}$$

$$\nabla^2\psi-\frac{1}{r^2}\psi-\frac{1}{\delta^2}\ddot{\psi}=\frac{p}{\delta^2}\phi, \tag{14}$$

$$\nabla^2\phi-\frac{1}{r^2}\phi-2\delta^*\phi-\frac{1}{\delta_1^2}\ddot{\phi}=\delta^2\left(\nabla^2\psi-\frac{\psi}{r^2}\right), \tag{15}$$

$$\nabla^2T-\left(\frac{\partial T}{\partial t}+t_0\frac{\partial^2T}{\partial t^2}\right)=\varepsilon\nabla^2\left(\frac{\partial q}{\partial t}+\delta_{1k}t_0\frac{\partial^2q}{\partial t^2}\right), \tag{16}$$

$$\nabla^2\phi_j-\frac{1}{\delta_L^2(1+\varepsilon^*)}\frac{\partial^2\phi_j}{\partial t^2}=0,\quad j=1,2, \tag{17}$$

$$T_j=\frac{-\varepsilon^*\rho_L}{\bar{\beta}\rho(1+\varepsilon^*)}\frac{\partial^2\phi_j}{\partial t^2},\quad j=1,2 \tag{18}$$

where

$$T_j'=\frac{T_j}{T_0},\qquad \varepsilon^*=\frac{\beta^{*2}T_0^*}{\rho_LC_V^*c_L^2},\qquad \bar{\beta}=\frac{\beta^*}{\nu},$$

$$\beta^*=3\lambda_L\alpha^*,\qquad \delta_L^2=\frac{c_L^2}{c_1^2},\qquad c_L=\sqrt{\frac{\lambda_L}{\rho_L}}, \tag{19}$$

$$\nabla^2=\frac{\partial^2}{\partial r^2}+\frac{1}{r}\frac{\partial}{\partial r}+\frac{\partial^2}{\partial z^2}.$$

Here c_L is the velocity of sound in the liquid; λ_L is the bulk modulus, ρ_L is density of the liquid, α^* is the coefficient of volume thermal expansion; C_V^* is the specific heat of the fluid at constant volume; T_1 and T_2 are respectively the temperature deviations in the liquid layers below and above the thermoelastic micropolar plate from the ambient temperature T_0^* and ε^* is the thermomechanical coupling in the liquid. Moreover, the liquid is assumed to be thermally non-conducting hypothetical solid and the prime has been omitted for convenience.

2.1 Boundary conditions

The boundary conditions at the solid liquid interfaces $z=\pm d$ to be satisfied are as follows:

$$\begin{aligned}&\sigma_{zz}=\sigma_{zz}^L,\qquad \sigma_{zr}=\sigma_{zr}^L,\qquad w=w_L,\\ &m_{z\theta}=0,\qquad T_{,z}+H(T-T_j)=0,\quad j=1,2\end{aligned} \tag{20}$$

where H is the Biot's heat transfer coefficient.

3 Formal solution of the problem

We assume the solution of the form

$$\begin{aligned}&(q,\psi,T,\phi,\phi_1,\phi_2)\\ &\quad=\left\{\begin{matrix}q(z)J_0(\xi r),\psi(z)J_1(\xi r),T(z)J_0(\xi r),\\ \phi(z)J_1(\xi r),\phi_1(z)J_0(\xi r),\phi_2(z)J_0(\xi r)\end{matrix}\right\}\\ &\qquad\times\exp(-i\omega t)\end{aligned} \tag{21}$$

where $c=\frac{\omega}{\xi}$ is the non-dimensional phase velocity ($c'=\frac{c}{c_1}$), $\omega(\omega'=\frac{\omega}{\omega^*})$ is the non-dimensional circular frequency, ξ ($\xi'=\frac{c_1\xi}{\omega^*}$) the non-dimensional wave number; J_0 and J_1 are Bessel functions of order 0 and 1, respectively. Here primes have been suppressed.

Upon using solution (21) in (13) to (18) and solving the resulting coupled differential equations the expressions for q, ϕ, ψ, T, ϕ_1, ϕ_2, T_1 and T_2 are obtained as

$$\begin{aligned}q=&(A\cos m_1z+B\sin m_1z+C\cos m_2z+D\sin m_2z)\\ &\times J_0(\xi r)\exp(-i\omega t),\end{aligned} \tag{22}$$

$$\begin{aligned}\phi=&\frac{\delta^2}{p}[(\beta^2-m_3^2)(A'\cos m_3z+B'\sin m_3z)\\ &+(\beta^2-m_4^2)(C'\cos m_4z+D'\sin m_4z)]\\ &\times J_1(\xi r)\exp(-i\omega t),\end{aligned} \tag{23}$$

$$\begin{aligned}\psi=&(A'\cos m_3z+B'\sin m_3z+C'\cos m_4z\\ &+D'\sin m_4z)J_1(\xi r)\exp(-i\omega t),\end{aligned} \tag{24}$$

$$\begin{aligned}T=&i\omega^{-1}\tau^{-1}[(\alpha^2-m_1^2)(A\cos m_1z+B\sin m_1z)\\ &+(\alpha^2-m_2^2)(C\cos m_2z+D\sin m_2z)]\\ &\times J_0(\xi r)\exp(-i\omega t),\end{aligned} \tag{25}$$

$$\phi_1 = E\sin\gamma[z-(d+h)]J_0(\xi r)\exp(-i\omega t), \quad d<z<d+h, \tag{26a}$$

$$T_1 = \frac{\omega^2\varepsilon^*\rho_L}{\bar{\beta}\rho(1+\varepsilon^*)}E\sin\gamma[z-(d+h)] \times J_0(\xi r)\exp(-i\omega t), \quad d<z<d+h, \tag{26b}$$

$$\phi_2 = F\sin\gamma[z+(d+h)]J_0(\xi r)\exp(-i\omega t), \quad -(d+h)<z<d, \tag{27a}$$

$$T_2 = \frac{\omega^2\varepsilon^*\rho_L}{\bar{\beta}\rho(1+\varepsilon^*)}B_6\sin\gamma[z+(d+h)]J_0(\xi r) \times \exp(-i\omega t), \quad -(d+h)<z<d, \tag{27b}$$

where

$$m_k^2 = \xi^2(a_k^2c^2-1), \quad k=1,2,3,4,$$
$$\gamma^2 = \xi^2\left(\frac{c^2}{\delta_L^2}-1\right) = m_5^2, \qquad \alpha^2 = \xi^2(c^2-1),$$
$$\beta^2 = \xi^2\left(\frac{c^2}{\delta^2}-1\right),$$

$$\begin{aligned} u = \{&-\xi(A\cos m_1z + B\sin m_1z \\ &+ C\cos m_2z + D\sin m_2z) \\ &- m_3(A'\sin m_3z + B'\cos m_3z) \\ &- m_4(C'\sin m_4z - D'\cos m_4z)\}J_1(\xi r)e^{-i\omega t}, \\ w = [&-m_1(A\sin m_1z - B\cos m_1z) \\ &+ m_2(-C\sin m_2z + D\cos m_2z) \\ &- \xi(A'\cos m_3z + B'\sin m_3z \\ &+ C'\cos m_4z + D'\sin m_4z)]J_0(\xi r)e^{-i\omega t}, \end{aligned} \tag{28}$$

$$\begin{aligned} a_1^2, a_2^2 &= \frac{1}{2}[(1+\tau_0-i\omega\varepsilon\tau_0'\tau_1) \\ &\quad \pm[(1-\tau_0-i\omega\varepsilon\tau_0'\tau_1)^2 - 4i\omega\varepsilon\tau_0'\tau_1\tau_0]^{1/2}], \\ a_3^2, a_4^2 &= \frac{1}{2}\Bigg[\frac{1}{\delta^2}+\frac{1}{\delta_1^2}+\frac{\delta^*}{\delta^2\omega^2}(p-2\delta^2) \\ &\quad \pm\Bigg[\frac{1}{\delta^2}-\frac{1}{\delta_1^2}+\frac{\delta^*}{\delta^2\omega^2}(p-2\delta^2)^2 \\ &\quad + \frac{4\delta^*(p-2\delta^2+2\delta_1^2)}{\omega^2\delta^2\delta_1^2}\Bigg]^{1/2}\Bigg] \end{aligned} \tag{29}$$

where

$$\tau_0 = t_0 + i\omega^{-1}, \qquad \tau_0' = t_0\delta_1 k + i\omega^{-1}, \qquad \tau_1 = t_1\delta_{2k} + i\omega^{-1}. \tag{30}$$

4 Derivation of secular equations

Invoking the boundary conditions (20) at the surfaces $z=\pm d$ of the plate along with solutions (22)–(27) we obtain a system of 10 simultaneous linear equations which has a non-trivial solution if the determinant of unknown coefficients $[A, B, C, D, E, F, A', B', C', D']$ vanishes. Upon employing the procedure adopted by Graff [25, pp. 439–446], Wu and Zhu [20] in elastokinetics and Sharma and Pathania [21, 22] in thermoelasticity mechanics, after some algebraic reductions and manipulations along with conditions

$$\gamma \neq 0, \qquad \gamma h \neq (2n-1)\frac{\pi}{2}, \qquad m_i d \neq n\pi, \qquad (2n-1)\frac{\pi}{2}, \quad n=1,2,3,\ldots.$$

The system of equations leads to the following secular equations.

$$\begin{aligned} &\left(\frac{T_1}{T_3}\right)^{\pm1} - \frac{m_1(m_1^2-\alpha^2)}{m_2(m_2^2-\alpha^2)}\left(\frac{T_2}{T_3}\right)^{\pm1} \\ &\quad + \frac{\omega^4\rho_L m_1(m_2^2-m_1^2)T_5}{\rho\gamma(m_2^2-\alpha^2)[T_3]^{\pm1}P^2} \\ &\quad - \frac{m_1m_3(m_2^2-m_1^2)Q^2}{(m_2^2-\alpha^2)LP^2} \\ &= H\frac{m_3m_1Q^2}{m_2LP^2}\left[\frac{T_1T_2}{T_3}\right]^{\pm1} \\ &\quad \times\Bigg[\left(1-\frac{\omega^4\rho_LLT_5}{\rho\gamma Q^2m_3T_3^{\pm1}}\right)\left(\left(\frac{T_1}{T_3}\right)^{\mp1} \\ &\quad - \frac{m_2(m_1^2-\alpha^2)}{m_1(m_2^2-\alpha^2)}\left(\frac{T_2}{T_3}\right)^{\pm1}\right) \\ &\quad - \frac{(m_1^2-m_2^2)LP^2}{m_1m_3(\alpha^2-m_2^2)Q^2} \\ &\quad + \frac{i\omega^5\tau_1\varepsilon^*LT_5\rho_L}{\bar{\beta}(1+\varepsilon^*)\gamma(\alpha^2-m_2^2)\rho m_1m_3Q^2} \\ &\quad \times\left(\left(\frac{T_1}{T_3}\right)^{\mp1} - \frac{m_2}{m_1}\left(\frac{T_2}{T_3}\right)^{\mp1}\right)\Bigg] \end{aligned} \tag{31}$$

where $T_k = \tan m_k d$ $(k = 1, 2, 3, 4)$, $T_5 = \tan \gamma h$,

$$L = \frac{(1 - a_4^2\delta^2)}{(a_4^2 - a_3^2)\delta^2}\left[1 - \frac{m_3(1 - a_3^2\delta^2)[T_3]^{\pm 1}}{m_4(1 - a_4^2\delta^2)[T_4]^{\pm 1}}\right],$$

$$P = \delta^2\left(\beta^2 - \xi^2 + p\frac{\xi^2}{\delta^2}\right),$$

$$Q = 2\delta^2\xi\left(1 - \frac{p}{2\delta^2}\right), \qquad \alpha = \xi^2(c^2 - 1).$$

Here superscript $+1$ corresponds to skew symmetric and -1 refers to symmetric modes of wave propagation. Equation (31) is the secular equation which governs the propagation of circular crested micropolar generalized thermoelastic waves in a plate sandwiched between two inviscid liquid layers. The secular equation for such waves in a plate sandwiched between two liquid half spaces ($H \to \infty$) can be written from (31) by replacing $\tan \gamma h$ with $-i$. The former case may also be referred as non leaky Lamb type waves and latter one as leaky Lamb waves in micropolar generalized thermoelastic plates.

The secular equation in case of generalized thermoelastic plate and micropolar elastic plate immersed in liquid can be obtained by setting respectively $\kappa = 0 = p$ and $\varepsilon = 0$ in (31). The results for thermoelastic, elastic and micropolar elastic can also be obtained from secular (31) by taking $\rho_L \to 0$ along with above choice of thermoelastic coupling and micropolarity parameters. The deduced results agree with Sharma and Pathania [21, 22], Sharma and Singh [26], Sharma et al. [27] and Graff [25].

5 Plane waves in plate

In this section we consider a plane wave in infinite plate. We take origin of the Cartesian coordinate system (x, y, z) on the middle surface of the plate. The x–y plane is chosen to coincide with the middle surface of the plate and z-axis normal to it along the thickness of the plate. The surfaces $z = \pm d$ are assumed to be stress free, thermally insulated or isothermal boundaries of the plate. The non-dimensional basic governing equations of micropolar generalized thermoelasticity in this case are again given by (13) to (18) with $\nabla^2 = \frac{\partial^2}{\partial x^2} + \frac{\partial^2}{\partial z^2}$, $x' = \frac{\omega^* x}{c_1}$ and the operator ∇ is in Cartesian coordinates instead of cylindrical one here.

The boundary conditions at the solid liquid interfaces $z = \pm d$ to be satisfied are as follows:

$$\begin{aligned} &\sigma_{zz} = \sigma_{zz}^L, \qquad \sigma_{zy} = \sigma_{zy}^L, \\ &w = w_L, \qquad m_{zy} = 0, \\ &T_{,z} + H(T - T_j) = 0, \quad j = 1, 2 \end{aligned} \tag{32}$$

and the potential functions q and ψ in the solid defined by

$$u = q_{,x} + \psi_{,z}, \qquad w = q_{,z} - \psi_{,x} \tag{33}$$

where q and ψ are velocity potential function of longitudinal and shear waves in the solid plate Substituting expressions (33) in (8) to (10), we obtained

$$\left(\nabla^2 - \frac{\partial^2}{\partial t^2}\right)q = \left(1 + t_1\delta_{2k}\frac{\partial}{\partial t}\right)T, \tag{34}$$

$$\nabla^2\psi - \frac{1}{\delta^2}\ddot{\psi} = \frac{p}{\delta^2}\phi, \tag{35}$$

$$\nabla^2\phi - 2\delta^*\phi - \frac{1}{\delta_1^2}\ddot{\phi} - \delta^2\nabla^2\psi = 0, \tag{36}$$

$$\nabla^2 T - \left(\frac{\partial T}{\partial t} + t_0\frac{\partial^2 T}{\partial t^2}\right) = \varepsilon\nabla^2\left(\frac{\partial q}{\partial t} + \delta_{1k}t_0\frac{\partial^2 q}{\partial t^2}\right). \tag{37}$$

In the fluid medium, we have

$$u_1 = \phi_{1,x} + \psi_{1,z}, \qquad w_1 = \phi_{1,z} - \psi_{1,x} \tag{38}$$

where ϕ_1 and ψ_1 are the scalar and vector velocity potential, u_1 and w_1 are the x and z components of particle velocity in the medium, respectively. Because the inviscid liquid does not support the shear motion so shear modulus of liquid vanishes and hence $\psi_1 = 0$. The potential function ϕ_1 in the case of liquid satisfies the equation

$$\begin{aligned} &\nabla^2\phi_j - \frac{1}{\delta_L^2(1 + \varepsilon^*)}\ddot{\phi}_j = 0, \quad j = 1, 2, \\ &T_j = \frac{-\varepsilon^*\rho_L}{\bar{\beta}\rho(1 + \varepsilon^*)}\ddot{\phi}_j, \quad j = 1, 2 \end{aligned} \tag{39}$$

where $\delta_L^2 = \frac{c_L^2}{c_1^2}$, $c_L = \sqrt{\frac{\lambda_L}{\rho_L}}$ being velocity of sound in liquid. Here ρ_L is the density and λ_L is bulk modulus of the liquid.

Here we take the wave solution of the form

$$(q, \psi, T, \phi, \phi_1, \phi_2) = \{q(z), \psi(z), T(z), \phi(z), \phi_1(z), \phi_2(z)\} \times \exp(i\xi(x - ct)). \tag{40}$$

Upon using solution (40) in (34) to (39) the formal solution in this case is obtained as

$$q = (A^* \cos m_1 z + B^* \sin m_1 z + C^* \cos m_2 z + D^* \sin m_2 z) \exp(i\xi(x - ct)), \tag{41}$$

$$\phi = \frac{\delta^2}{p}[(\beta^2 - m_3^2)(A'^* \cos m_3 z + B'^* \sin m_3 z) + (\beta^2 - m_4^2)(C'^* \cos m_4 z + D'^* \sin m_4 z)] \times \exp(i\xi(x - ct)), \tag{42}$$

$$\psi = (A'^* \cos m_3 z + B'^* \sin m_3 z + C'^* \cos m_4 z + D'^* \sin m_4 z), \exp(i\xi(x - ct)), \tag{43}$$

$$T = i\omega^{-1}\tau^{-1}[(\alpha^2 - m_1^2)(A^* \cos m_1 z + B^* \sin m_1 z) + (\alpha^2 - m_2^2)(C^* \cos m_2 z + D^* \sin m_2 z)] \times \exp(i\xi(x - ct)), \tag{44}$$

$$\phi_1 = E^* \sin \gamma[z - (d + h)] \exp(i\xi(x - ct)), \quad d < z < d + h,$$

$$T_1 = \frac{\omega^2 \varepsilon^* \rho_L}{\bar{\beta}\rho(1 + \varepsilon^*)} E^* \sin \gamma[z - (d + h)] \times \exp(i\xi(x - ct)), \quad d < z < d + h, \tag{45}$$

$$\phi_2 = F^* \sin \gamma[z + (d + h)] \exp(i\xi(x - ct)), \quad -(d + h) < z < d,$$

$$T_2 = \frac{\omega^2 \varepsilon^* \rho_L}{\bar{\beta}\rho(1 + \varepsilon^*)} F^* \sin \gamma[z + (d + h)] \times \exp(i\xi(x - ct)), \quad -(d + h) < z < d, \tag{46}$$

where m_i, a_i; $i = 1, 2, 3, 4$, etc. are defined in (28) and (29). Upon invoking boundary conditions (32) at the plate surfaces $z = \pm d$ and using (41)–(46), we obtain a coupled system of twelve simultaneous linear equations which provides a non-trivial solution if the determinant of the amplitudes $[A^*, B^*, C^*, D^*, E^*, F^*, A'^* B'^*, C'^*, D'^*]$ vanishes. The determinant equation so obtained, after applying lengthy reductions and manipulations, again leads to the secular equation (31) for the micropolar generalized thermoelastic rectangular plate bordered both on the top and bottom with infinitely large homogeneous inviscid liquid layers of thickness h with stress free isothermal and thermally insulated boundaries.

Therefore it is noticed that the Rayleigh–Lamb type equation governs plane wave motion in a micropolar generalized thermoelastic plate as in case of elastokinetics and thermo mechanics. Although, the frequency wave number relationship holds whether waves are straight or circularly crested, the displacements, temperature change, stresses and couple stress in case of crested waves vary according to Bessel functions rather than trigonometric functions as far as the radial coordinate is concerned. For large values of r, we have

$$J_0(\xi r) \to \frac{\sin \xi r + \cos \xi r}{\sqrt{\pi \xi r}},$$

$$J_1(\xi r) = \frac{\sin \xi r - \cos \xi r}{\sqrt{\pi \xi r}}.$$

Thus far from the origin the motion becomes periodic in r. Actually "far" occurs rather rapidly, within four to five zeros of Bessel functions. As r becomes very large the straight crested behavior is the limit of circular crested waves.

6 Discussion of the secular equations

6.1 Wave of short wave length

Let us consider the case when the transverse wavelength with respect to the thickness of the plate is quite small, so that $\xi d \geq 1$. In this case the characteristic roots are of the type $\alpha^2 = -\alpha'^2$, $\beta^2 = -\beta'^2$, $m_k^2 = -m_k'^2$, $k = 1, 2, 3, 4$ so that $m_k = i\alpha_k$, $k = 1, 2, 3, 4$ are purely imaginary or complex numbers. This ensures that the superposition of partial waves has the property of exponential decay. The secular equation is written from (31) by replacing circular tangent functions of α, β and m_k, $k = 1, 2, 3, 4$ with hyperbolic tangent function of α', β' and α_k $(k = 1, 2, 3, 4)$ and some information on the asymptotic behavior is also obtainable by putting $\xi d \to \infty$, $\frac{\tanh \alpha_k d}{\tanh \alpha_3 d} \to 1$, $k = 1, 2$ so that the resulting frequency equation reduces to

$$A\Big[\alpha_1^2 + \alpha_2^2 + \alpha_1 \alpha_2 - \alpha'^2$$

$$\mp \frac{i\omega^2\delta^2(-\beta'^2+\xi^2)(\alpha_1+\alpha_2)\rho_L\alpha_1\alpha_2\tan\gamma h}{\rho\gamma P^2}\Bigg]$$
$$+\alpha_1\alpha_2\alpha_3\frac{(a_4^2-a_3^2)(\alpha_1+\alpha_2)\delta^2Q^2}{(1-a_4^2\delta^2)P^2}$$
$$=\pm H\frac{\alpha_3(a_4^2-a_3^2)\delta^2Q^2}{(1-a_4^2\delta^2)P^2}$$
$$\times\Bigg[\Bigg(1\mp\frac{i\omega^2\rho_L(-\beta'^2+\xi^2)(1-a_4^2\delta^2)\tan\gamma h}{\rho\gamma\alpha_3(a_4^2-a_3^2)Q^2}\Bigg)$$
$$\times(\alpha_1\alpha_2-\alpha'^2)$$
$$+\frac{(1-a_4^2\delta^2)(\alpha_1+\alpha_2)P^2A}{(a_4^2-a_3^2)\delta^2Q^2}$$
$$\pm i\frac{\omega^4\varepsilon^*(1-a_4^2\delta^2)\tan\gamma h}{\bar\beta(1+\varepsilon^*)\gamma(a_4^2-a_3^2)\alpha_3Q^2}\Bigg],$$
$$A=\Bigg[1-\frac{\alpha_3(1-m_3\delta^2)}{\alpha_4(1-m_4\delta^2)}\Bigg]. \tag{47}$$

Equation (47) is the dispersion equation for micropolar thermoelastic Rayleigh waves of an infinite half-space solid bordered with a homogeneous liquid layer of finite thickness. The dispersion relation in case of Rayleigh waves of an infinite solid half-space underlying a homogeneous liquid half space is written from (47) by replacing $\tan\gamma h$ with 1 therein. The results of classical thermoelastic plate can be obtained by ignoring the micropolar effect.

6.2 Long wavelength waves

Let us consider the case when the transverse wave length with respect to thickness to the plate is quite large $\xi d\le 1$. When the characteristic roots are of the type $\alpha^2=-\alpha'^2$, $\beta^2=-\beta'^2$, $m_k^2=-m_k'^2$, $k=1,2,3,4$ so that $\alpha=i\alpha'$, $\beta=i\beta'$, $m_k=i\alpha_k$, $k=1,2,3,4$ are purely imaginary or complex numbers. In this case the symmetric case has no root. The skew symmetric case on retaining the first two terms in the expansion of hyperbolic tangents and frequency $(H\to 0)$ reduces to

$$(\alpha_3^2+\alpha_4^2-\beta'^2)\Bigg(\beta'^2+\xi^2-p\frac{\xi^2}{\delta^2}\Bigg)^2$$
$$\times\Bigg(1-\frac{d^2}{3}\Bigg(\frac{\alpha_3^4+\alpha_4^4+\alpha_3^2\alpha_4^2-\beta'^2(\alpha_3^2+\alpha_4^2)}{\alpha_3^2+\alpha_4^2-\beta'^2}\Bigg)$$
$$\times\Bigg(1-\frac{\alpha'^2d^2}{3}+\frac{\omega^2\rho_L(\xi^2-\beta'^2)\tan\gamma h}{\rho d\gamma\delta^2}\Bigg)$$
$$=4\xi^2\Bigg(1-\frac{p}{2\delta^2}\Bigg)\alpha_3^2\alpha_4^2\Bigg(1-\alpha_3^2\frac{d^2}{3}\Bigg)\Bigg(1-\alpha_4^2\frac{d^2}{3}\Bigg). \tag{48}$$

On discarding the terms of higher order than $(\frac{c}{\delta})^4$, we get

$$c=2\xi d\delta\sqrt{\frac{(1-\frac{p}{2\delta^2})\{(3-\delta^2)(1-\frac{p}{2\delta^2})-2\}}{3}}$$
$$\times\Bigg\{1-\frac{\rho_Lh}{\rho d^2}+4\delta^2\Bigg(1-\frac{p}{2\delta^2}\Bigg)$$
$$\times\Bigg[\Bigg(a_3^2+a_4^2-\frac{1}{\delta^2}\Bigg)$$
$$-\delta^2\Bigg(1-\frac{p}{2\delta^2}\Bigg)a_3^2a_4^2\Bigg]\Bigg\}^{-1/2}. \tag{49}$$

In the absence of micropolarity $(p\to 0)$, (49) becomes

$$c=2\xi d\delta\sqrt{\frac{1-\delta^2}{3}}\Bigg\{1-\frac{\rho_Lh}{\rho d}\Bigg\}^{-1/2}. \tag{50}$$

This agrees with Sharma and Pathania [22]. In the absence of liquid $(\rho_L\to 0)$, (50) reduces to

$$c=2\xi d\delta\Bigg[\frac{1}{3}(1-\delta)^2\Bigg]^{1/2}. \tag{51}$$

This result with linear dependence of c on ξ agrees with that derived from classical plate theory in elastokinetics. From (49)–(51) it has been observed that thermomechanical coupling or thermal relaxation time are not affecting thin plates in this case. How ever the presence of liquid on both sides of the plate and micropolarity affects the phase velocity of flexural vibration mode as a periodic function of liquid layer width.

When two of the characteristic roots are of the type $\alpha^2=-\alpha'^2$, $m_k^2=-m_k'^2$, $k=1,2$, then the frequency equation can be obtained from (31) by replacing only the circular tangent functions of m_k, $k=1,2$ with hyperbolic tangent functions. In this case the antisymmetric case no roots and secular equation in the symmetric case becomes

$$(\alpha_1^2+\alpha_2^2-\alpha'^2)-\frac{\omega^2\rho_L(\beta^2+\xi^2)\alpha_1^2\alpha_2^2d\tan\gamma h}{\rho\gamma\delta^2(\beta^2-\xi^2+\frac{p\xi^2}{\delta^2})^2}$$

$$= \frac{4\xi^2(1-\frac{p}{2\delta^2})\alpha_1^2\alpha_2^2}{(\beta^2-\xi^2+p\frac{\xi^2}{\delta^2})^2}. \tag{52}$$

This on simplification provides us

$$c = \frac{2\delta\sqrt{(1-\delta^2)(1-\frac{p}{2\delta^2})(1+\frac{p}{2(1-\delta^2)})}}{\sqrt{1+4\delta^2(1-\frac{p}{2\delta^2})(a_1^2+a_2^2-1)-4\delta^2a_1^2a_2^2(1-\frac{p}{2\delta^2})^2-\frac{\rho_L h\xi^2 d}{\rho\delta^2}}}. \tag{53}$$

In the absence of micro polarity ($\kappa = 0 = p$), (53) reduces to

$$c = \frac{2\delta\sqrt{(1-\delta^2)}}{\sqrt{1-4i\omega\delta^2\varepsilon\tau_0'\tau_1-\frac{\rho_L h\xi^2 d}{\rho\delta^2}}}. \tag{54}$$

This in case of coupled thermoelasticity becomes

$$c = \frac{2\delta\sqrt{(1-\delta^2)}}{\sqrt{1+4i\omega^{-1}\delta^2\varepsilon}}. \tag{55}$$

The above equation in uncoupled thermoelasticity ($\varepsilon = 0$) further reduces to

$$c = 2\delta\sqrt{(1-\delta^2)}. \tag{56}$$

This is the thin plate or plane stress analogue of bar velocity of longitudinal rod theory in elastokinetics; see Graff [25]. This shows that thin plate results in this mode are affected by thermoelastic coupling and thermal relaxation times.

7 Numerical results and discussion

Following Gauthier [28] the relevant physical constants for aluminum-epoxy composite as micropolar elastic solid are

$\rho = 2.19 \times 10^3$ kg/m^3, $\lambda = 7.59 \times 10^{10}$ N/m^2,

$\mu = 1.89 \times 10^{10}$ N/m^2, $T_0 = 20°$C,

$\kappa = 0.0149 \times 10^{10}$ N/m^2, $\gamma = 0.268 \times 10^6$ N,

$j = 0.196 \times 10^{-4}$ m^2, $\bar{\beta} = 280$,

$t_0 = 0.6131 \times 10^{-13}$ s, $t_1 = 0.8765 \times 10^{-13}$ s,

$\varepsilon = 0.073$, $\frac{\omega}{\omega_0^2} = 10$.

Table 1 Specific heat of water at different temperatures

T_0^* (°C)	0	15	35	50	100
C_V^* (J/kg °C)	1.008	1.00	0.997	0.998	1.006

Here the values of the thermal relaxation time t_0 have been estimated from (2.5) of Chandrasekharaiah [16] and the values of t_1 are taken proportional to that of t_0. The fluid taken for the purpose of numerical discussion is water, the velocity of sound in which is $c_L = 1.5 \times 10^3$ m/s and density $\rho_L = 1000$ kg/m^3. The specific heat of water at different temperatures is given in Table 1.

In general, wave number (ξ) and hence the phase velocity (c) of the wave is complex quantity. We write

$$c^{-1} = V^{-1} + i\omega^{-1}Q \tag{57}$$

so that $\xi = R + iQ$, $R = \frac{\omega}{V}$, where V and Q are real. The exponent in the plane wave solution (40) becomes $iR(x - Vt) - Qx$. This shows that V is the propagation speed and Q is the attenuation coefficient of the waves. The complex secular (31) is solved via representation (57) by using functional iteration numerical technique to compute phase speed (V) and attenuation coefficient (Q) of Lamb waves for different values of the wave number (R) for micropolar thermoelastic (MPT) and thermoelastic (TE) solid plates.

Here the specific loss of energy (SL) and relative frequency shift (RFS) are also computed. The specific loss is the rate of energy dissipation ($\frac{\Delta W}{W}$) in a stress cycle of the specimen when the strain is maximal, W being the strain energy density function. It is given by

$$\left|\frac{\Delta W}{W}\right| = 4\pi\left|\frac{\mathrm{Im}(\xi)}{\mathrm{Re}(\xi)}\right|,$$

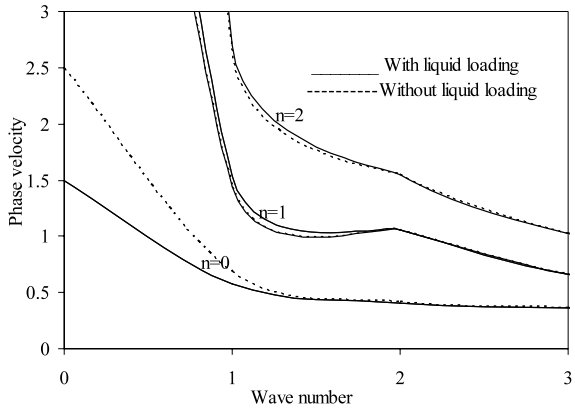

Fig. 1 Phase velocity profiles of symmetric modes with wave number in micropolar thermoelastic plate (MPT) plate

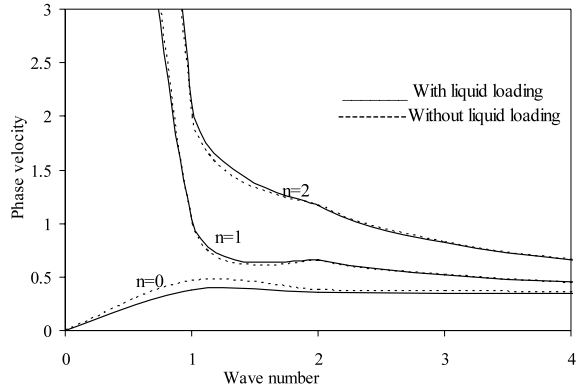

Fig. 2 Phase velocity profiles of asymmetric modes with wave number in micropolar thermoelastic plate (MPT) plate

ξ being complex. Here we have

$$\mathrm{SL} = \left|\frac{\Delta W}{W}\right| = 4\pi \left|\frac{VQ}{\omega}\right|. \tag{58}$$

The relative frequency shift is defined by the relation as given below

$$\mathrm{RFS} = \left|\frac{\omega(\rho_L) - \omega(0)}{\omega(0)}\right| \tag{59}$$

where $\omega(\rho_L)$, $\omega(0)$ are the frequencies in the presence and absence of fluid loading, respectively. The computer simulated results have been presented graphically in Figs. 1 to 12.

From Fig. 1 it is observed that phase velocity of the lowest symmetrical mode in micropolar thermoelastic plate is significantly reduced and affected in the presence of liquid in the wave number range $0 \leq R \leq 1.5$ and it exhibits non-dispersive behavior for $R \geq 1.5$. The phase velocity of higher modes attain large values at small wave numbers which approaches asymptotically to the thermoelastic Rayleigh wave velocity with increasing wave number.

It is observed from Fig. 2 that the phase velocity of lowest asymmetric mode increases from zero value at vanishing wave number to become closer to the velocity of thermoelastic Rayleigh wave at large wave numbers. It is also reduced and affected due to presence of liquid. For optical modes the phase velocity is quite large at vanishing wave number which again approaches asymptotically to thermoelastic Rayleigh wave velocity as experienced in the case of symmetric mode. This asymptotic behavior is attributed to the

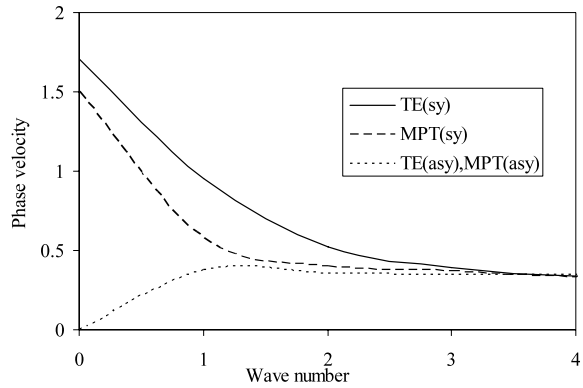

Fig. 3 Phase velocity profiles of fundamental modes (symmetric and asymmetric) with wave number in thermoelastic (TE) and micropolar thermoelastic plates (MPT) plates

fact that for short wavelengths, the material plate behaves like a thick slab and hence coupling between upper and lower boundaries is reduced because of which the symmetric and asymmetric motion of the plate becomes more and more similar. This behavior of phase velocity profiles of symmetric and skew symmetric modes agrees with that of thermoelastic plate bordered with liquid layers of inviscid liquid at uniform temperature (Sharma and Pathania [17]) except slight changes in magnitudes.

In view of the importance of the fundamental mode in various applications like liquid sensors, NDT, corrosion testing etc. comparison of both symmetrical and asymmetrical modes has been given in Fig. 3 in cases of micropolar thermoelastic and thermoelastic material plates in the context of non-classical theory of thermoelasticity (GL theory) under fluid loadings. It

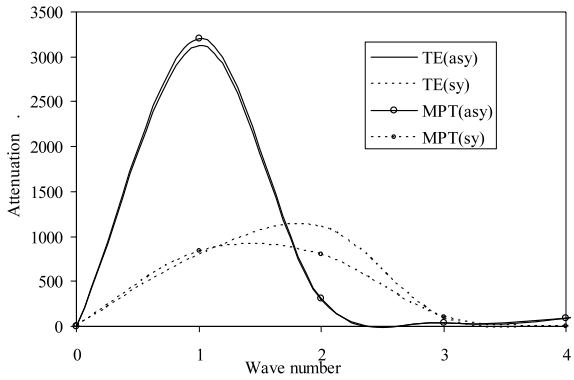

Fig. 4 Attenuation profile of fundamental modes (symmetric and asymmetric) with wave number in thermoelastic (TE) and micropolar thermoelastic (MPT) plates

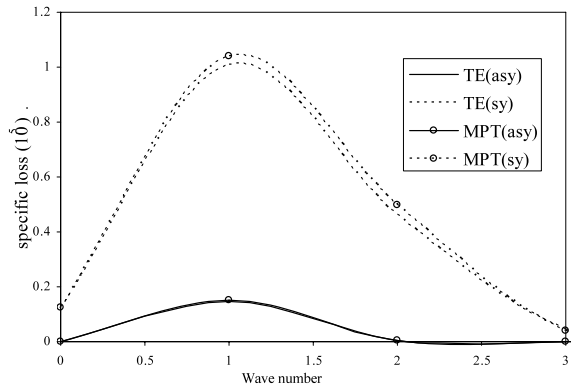

Fig. 5 Specific loss profile of fundamental modes (symmetric and asymmetric) with wave number in thermoelastic (TE) and micropolar thermoelastic plates (MPT) plates

has been observed that phase velocity of symmetric acoustic modes gets reduced in magnitude considerably because of the micropolar effects. However, symmetrical modes for both classes of material plates are behaving alike hence remains unaffected due to micropolarity.

Variations of attenuation of fundamental (acoustic) modes for both symmetric and skew symmetric have been plotted in Fig. 4 with respect to wave number in the presence and in absence of micropolar effects in thermoelastic plates. The magnitude of attenuation of asymmetric mode behaves in Gaussian manner with its maximum value at $R = 1$ in the wave number range $0 \leq R \leq 2.5$ and remains dispersionless afterwards. The behavior of this quantity in case of symmetric modes is also noticed to be Gaussian with maximum value at $R = 5$ for MPT (symmetrical) and at $R = 2$ for TE (symmetrical) in the wave number range $0 \leq R \leq 3.5$, however the latter is slightly platokurtic towards increasing wave number values. The magnitude of attenuation in case of symmetric modes is atleast about one-third times to that of skew symmetric ones. Moreover, the attenuation of skew symmetric modes increases due to micropolarity while it decreases in case of symmetric motion of the plate.

Figure 5 represents the behavior of specific loss factor of energy dissipation of symmetric and asymmetric modes with respect to wave number. The specific loss is noticed to be significant in the wave number range $0 \leq R \leq 2$ for asymmetric motion and in the range $0 \leq R \leq 3$ for symmetric motion of the plate. These profiles exhibit Gaussian behavior with peak values at $R = 1$ in both cases of the motion. However, the specific loss is one-sixth time less in case of asymmetric

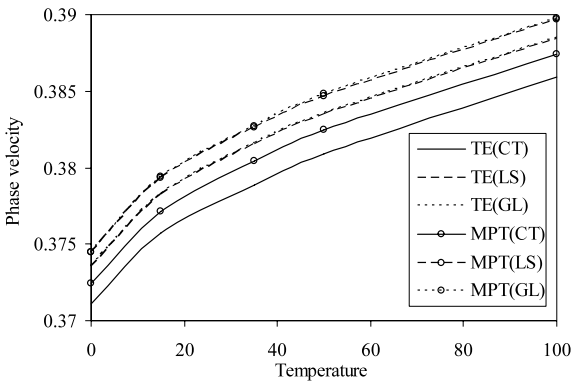

Fig. 6 Phase velocity profile of fundamental modes (symmetric and asymmetric) with ambient temperature of liquid medium in thermoelastic (TE) and micropolar thermoelastic (MPT) plates

mode as compared to symmetric one. Thus asymmetrical modes are more viable for practical applications.

The variations of phase velocity and attenuation of asymmetric modes with respect to liquid layer temperature are plotted in Figs. 6 and 7 respectively for different theories of non-classical elasticity viz. (CT, LS and GL). It is noticed that phase velocity increases monotonically with increasing liquid temperature in the considered material plates. The magnitude of this quantity increases both due to micropolarity as well as thermal relaxation time. It is obvious from Fig. 7 that the attenuation coefficient also increases monotonically with increasing liquid layer temperature; however profiles become stable and steady at higher temperature of the liquid loading. The magnitude of attenuation decreases both due to micropolarity and thermal relaxation effect. The effect of thermal relaxation

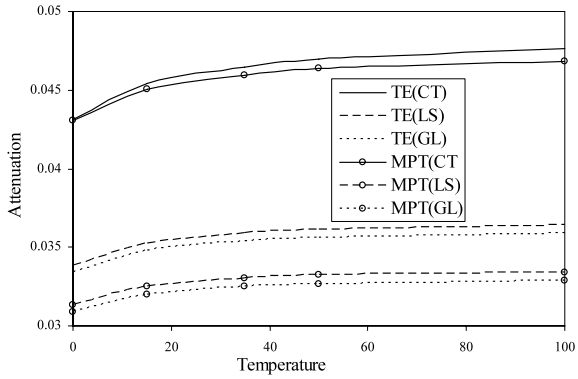

Fig. 7 Attenuation profile of fundamental modes (symmetric and asymmetric) with ambient temperature of liquid medium in thermoelastic (TE) and micropolar thermoelastic (MPT) plates

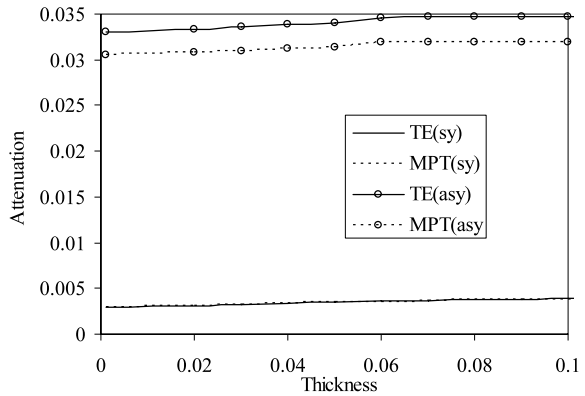

Fig. 9 Attenuation profiles of fundamental modes (symmetric and asymmetric) with respect to layer thickness of liquid layer in thermoelastic (TE) and micropolar thermoelastic (MPT) plates

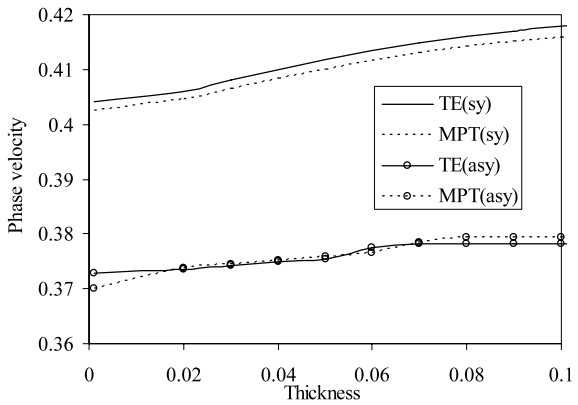

Fig. 8 Phase velocity profiles of fundamental modes (symmetrical and asymmetrical) with respect to thickness of liquid layer in thermoelastic (TE) and micropolar thermoelastic (MPT) plates

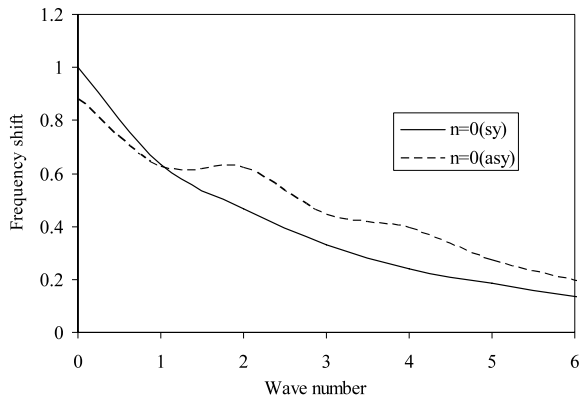

Fig. 10 Relative frequency shifts of fundamental modes (symmetric and asymmetric) due to fluid loading with wave number in micropolar thermoelastic plates (MPT) plate

is quite significant on the attenuation as compared to that on the phase velocity at all values of the liquid loading temperature.

The variations of phase velocity and attenuation coefficient of symmetric and skew symmetric motion of the plates with respect to liquid layer thickness are plotted in Figs. 8 and 9 respectively. It is noticed that magnitudes of both phase velocity and attenuation coefficient increases monotonically with increasing liquid layer thickness. The magnitude of phase velocity is slightly large in case of symmetric motion of the plate as compared to asymmetric one, though micropolarity results in reduction of phase velocity magnitude at all thickness values in case of former and in the range $0 \leq d \leq 0.02$ for asymmetric one. The phase velocity of asymmetric mode increases due to micropolarity for $d \geq 0.02$. The magnitude of attenuation in case of skew symmetric motion of the plate is slightly more as compared to symmetric one. The micropolarity results in decreasing the magnitudes of attenuation for both asymmetrical and symmetrical though very small in case of symmetric modes.

In Fig. 10 the relative frequency shift due to liquid loading of the plate is plotted with respect to wave number in case of symmetric and skew symmetric motion of the plate. The frequency shift decreases monotonically in both the cases with increasing wave numbers (decreasing wave lengths). However the profiles of relative frequency shift in case of symmetrical motion is smooth while that of skew symmetric is sub-

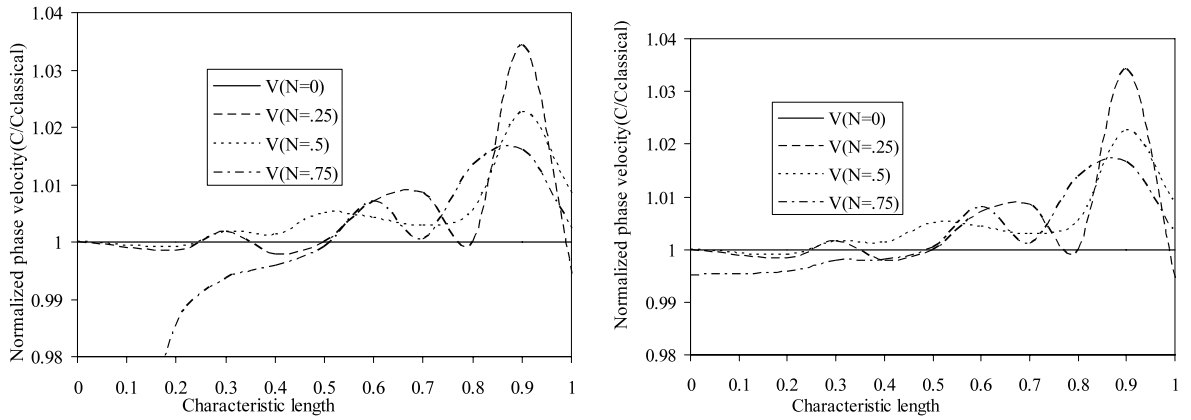

Fig. 11 (**a**) Phase velocity profile of acoustic symmetric mode with characteristic length for different values of coupling factor under free conditions (Normalized with classical value). (**b**) Phase velocity profile of acoustic symmetric mode with characteristic length for different values of coupling factor under fluid loading (normalized with classical value)

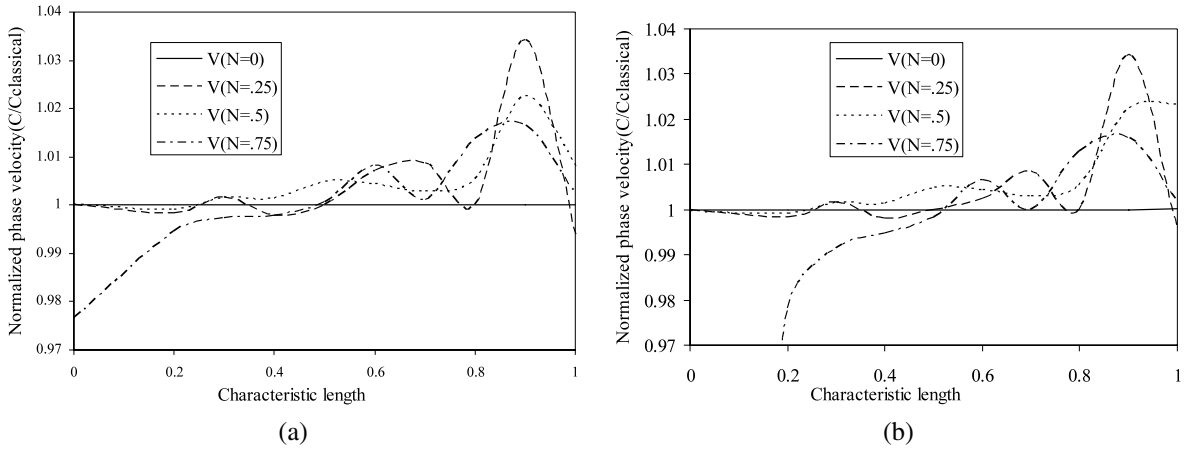

Fig. 12 (**a**) Phase velocity profile of acoustic asymmetric mode with characteristic length for different values of coupling factor under free conditions (normalized with classical value). (**b**) Phase velocity profile of acoustic asymmetric mode with characteristic length for different values of coupling factor under fluid loading (normalized with classical value)

jected to many sign reversals throughout the thickness of the plate.

The phase velocity profile of symmetric acoustical modes have been plotted for different values of coupling factor with respect to characteristic length in Figs. 11(a) and 11(b) under free and fluid loaded conditions. In order to have estimate of the polarity effects the normalization of the profiles have been done with respect to its corresponding classical values under free conditions. Phase velocity profiles show dispersion at higher values of characteristic lengths and coupling factors. Maximum dispersion is obtained at $l = 0.9$. At lower characteristic lengths phase velocities are less than their corresponding classical values for all curves. However a significant decrease is observed in case of profile corresponding to $N = 0.75$ an impact of coupling factor. Though phase velocities are quite similar to the profiles in the absence of fluid loading for $N = 0, 0.25, 0.5$ a significant effect of fluid loading has been observed for the profiles corresponding to for $N = 0.75$ at smaller characteristic lengths as phase velocity increases considerably.

Figures 12(a) and 12(b) show the phase velocity profiles of asymmetric acoustical modes for different

values of coupling factor with respect to characteristic length. The profiles are again normalized with their corresponding classical values under free conditions. Phase velocity profiles show dispersion at higher values of characteristic lengths and coupling factors. Maximum dispersion occurred obtained at $l = 0.9$. At small values of the characteristic lengths the phase velocity has smaller values than their corresponding classical values in each case. However a significant decrease in the magnitude of deviation is observed in case of the profile corresponding to $N = 0.75$ which clearly depicts the impact of coupling factor. Though phase velocity profiles are quite similar to the profiles in the absence of fluid loading for $N = 0$, 0.25, 0.5 a significant effect of fluid loading has been observed in case of $N = 0.75$ at smaller characteristic lengths.

8 Conclusions

Significant effect of fluid loading is observed on the phase velocity, attenuation coefficient and specific loss factor of symmetric and asymmetric modes of wave propagation in micropolar thermoelastic plates. Though in case of optical modes the phase velocity profiles for symmetrical and asymmetrical modes are in good agreement, they behave differently for acoustic modes. It has been observed that the phase velocity of symmetric acoustic mode considerably gets reduced in magnitude because of micropolar effects. The magnitude of attenuation in case of symmetric modes is about one-third times to that of skew symmetric ones. The attenuation of skew symmetric modes increases due to micropolarity while it decreases in case of symmetric motion of the plate. The specific loss is one-sixth times less in case of asymmetric modes as compared to symmetric one. When studied with respect to liquid loading temperature, the magnitudes of phase velocity and attenuation both increase due to micropolarity as well as thermal relaxation time. Though, the effect of thermal relaxation is quite significant on the attenuation as compared to that on the phase velocity at all values of the liquid loading temperature. Magnitudes of both phase velocity and attenuation coefficient increases monotonically with increasing liquid layer thickness. The magnitude of attenuation in case of skew symmetric motion of the plate is slightly more as compared to symmetric one. The micropolarity results in decreasing the magnitudes of attenuation for both asymmetrical and symmetrical though very small in case of symmetric modes. Significant effect of characteristic length and coupling factor has been observed on phase velocities. The instant study is useful in infrastructural health monitoring and may find applications in aerospace, navigation, civil engineering structures, chemical pipes, and automobiles industry. In biomedical engineering this model can be extended to model complex system of bones (micropolar) and prosthesis (elastic) in contact with fluids (blood etc.).

Acknowledgements The author (J.N.S.) is grateful to the University Grants Commission, New Delhi for providing financial support via project grant no. F. 30-236/2004(SR) to complete this work. The deep interest taken in this work and valuable suggestions made by the reviewer and Professor Vincenzo Parenti Castelli (Editor) are highly appreciated and thankfully acknowledged.

References

1. Voigt W (1887) Theoretishe studien uber die ebsti-Zitatsverhaltnisse der Kristalle. Abh Ges Wiss Gottingen 34
2. Cosserat E, Cosserat F (1909) Theorie des corps deformable. Hermann, Paris
3. Eringen AC, Suhubi ES (1964) Nonlinear theory of simple micro-elastic solids. Int J Eng Sci 2:189–203
4. Mindlin RD (1964) Microstructure in linear elasticity. Arch Ration Mech Anal 16:51–78
5. Eringen AC (1966) Linear theory of micropolar elasticity. J Math Mech 15:909–923
6. Fatemi J, Van Keulen F, Onck PR (2002) Generalized continuum theories: application to stress analysis in bone. Meccanica 37:385–396
7. Anderson WB, Lakes RS (1994) Size effects due to Cosserat elasticity and surface damage in closed-cell polymethacrylimide foam. J Mater Sci 29:6413–6419
8. Di Carlo A, Rizzi N, Tatone A (1990) Continuum modelling of beam like latticed truss: identification of the constitutive functions for the contact and inertial actions. Meccanica 25:168–174
9. Masiani R, Rizzi N, Trovalusci P (1995) Masonry as structured continuum. Meccanica 30:673–683
10. Masiani R, Trovalusci P (1996) Cauchy and Cosserat materials as continuum models of brick masonry. Meccanica 31:421–432
11. Lord HW, Shulman Y (1967) The generalized dynamical theory of thermoelasticity. J Mech Phys Solids 15:299–307
12. Green AE, Lindsay KA (1972) Thermoelasticity. J Elast 2:1–7
13. Ackerman CC, Betman B, Fairbank HA, Guyer RA (1966) Second sound in helium. Phys Rev Lett 16:789–791
14. Guyer RA, Krumhansal JA (1966) Thermal conductivity, Second sound phonon hydrodynamics phenomenon in non metallic crystals. Phys Rev Lett 148:778–788

15. Ackerman CC, Overtone WC (1969) Second sound in helium-3. Phys Rev Lett 22:764–766
16. Chanderasekharaiah DS (1986) Thermoelasticity with second sound-a review. Appl Mech Rev 39:355–376
17. Dost S, Tabarrok B (1978) Generalized micropolar thermoelasticity. Int J Eng Sci 16:173–178
18. Eringen AC (1970) Foundation of micropolar thermoelasticity. Course of lectures No 23, CISM Udine Springer
19. Kumar R, Choudhary S (2003) Response of orthotropic micropolar elastic medium due to various sources. Meccanica 38:349–368
20. Wu J, Zhu Z (1992) The propagation of Lamb waves in a plate bordered with layers of a liquid. J Acoust Soc Am 91:861–867
21. Sharma JN, Pathania V (2003) Generalized thermoelastic Lamb waves in a plate bordered with layers of inviscid liquid. J Sound Vib 268:897–916
22. Sharma JN, Pathania V (2005) Crested waves in Thermoelastic plates Immersed in liquid. J Vib Control 11:347–370
23. Sharma JN, Kumar S, Sharma YD (2008) Propagation of Rayleigh surface waves in microstretch thermoelastic continua under inviscid fluid loadings. J Therm Stress 31:18–39
24. Strunin DV (2001) On characteristics times in generalized thermoelasticity. J Appl Math 68:816–817
25. Graff KF (1991) Wave motion in elastic solids. Dover, New York
26. Sharma JN, Singh D (2002) Circular crested thermoelastic waves in homogeneous isotropic plate. J Therm Stress 25:1179–1193
27. Sharma JN, Singh D, Kumar R (2000) Generalized thermoelastic waves in homogeneous isotropic thermoelastic plate. J Acoust Soc Am 108:848–851
28. Gauthier RD (1982) Experimental investigation on micropolar media. In: Brulin O, Hsieh RKT (eds) Mechanics of micropolar media. World Scientific, Singapore, pp 395–463